Pergamon

Deep-Sea Research I, Vol. 42, No. 11/12, pp. 1989–2004, 1995
Elsevier Science Ltd
Printed in Great Britain

0967–0637(95)00079–8

Preferential concentration of marine particles in isotropic turbulence

KYLE D. SQUIRES* and HIDEKATSU YAMAZAKI†‡

(*Received* 6 *May* 1994; *in revised form* 13 *March* 1995; *accepted* 3 *July* 1995)

Abstract—The effect of small-scale turbulence on marine and aquatic particle transport has traditionally been thought to act as a means for creating homogeneous distributions. However, previous numerical simulations of heavy particle transport in turbulent flows have shown that particles are preferentially concentrated by turbulence and that effects of preferential concentration are most pronounced for particle parameters comparable to the Kolmogorov scales. Therefore, the focus of the present work is examination of the preferential concentration of marine particles. Application of Kolmogorov scaling indicates that effects of preferential concentration may be important for marine particles with diameters of order 1 mm in the upper mixed layer. Numerical simulations of unstratified isotropic turbulence are then used to support the notion that preferential concentration of particles possessing material characteristics representative of those encountered in marine environments can occur. In the simulations, particles of order 1 mm diameter are idealized as rigid spheres with a density ratio of 1.005. Simulation results demonstrate preferential concentration with peak particle number densities ranging from 10 to 60 times the global mean value. Implications of preferential concentration are also discussed, together with the limitations of the approach employed in the present study.

1. INTRODUCTION

One of the most complex physical processes shaping upper ocean and freshwater aquatic environments is turbulence. Of the many areas in which turbulence is an important factor, it is the interaction between suspended particles and the surrounding turbulent flow which is the focus of this work. Though the interactions are numerous and complicated, an improved fundamental understanding of the physical processes governing particle–turbulence interactions is needed and will ultimately shed new light on problems of biological and physical coupling.

In considering the range of interactions between turbulence and particles, one of the most fundamental issues is simply the influence of a turbulent environment on particle transport. For example, does turbulence act simply as a means of maintaining a homogeneous distribution of particles within a flow? This question and the associated areas of research constitute an important subset in the growing field of determining the influence of

*Mechanical Engineering Department, University of Vermont, Burlington, VT 05405-0156, U.S.A.
e-mail: squires @emba.uvm.edu.
†Department of Marine Science and Technology, Tokyo University of Fisheries, 4-5-7 Konan, Minato-ku, Tokyo 108, Japan.
‡Center for Earth and Ocean Research, University of Victoria, P.O. Box 1700, Victoria, B.C., Canada V8W 2Y2.

turbulence on plankton ecosystems (e.g., see Costello *et al.*, 1990; Marrase *et al.*, 1990; Mann and Lazier, 1991; Yamazaki and Kamykowski, 1991; Granata and Dickey, 1991; Madden and Day, 1992; Kiørboe, 1993).

It is noteworthy that the present understanding of turbulence incorporated into most aspects of marine and freshwater biology is that turbulence has an essentially random effect on transport. This view is predicated on the assumption that transport in a turbulent flow is similar to molecular transport and diffusion and is consequently reflected in plankton transport models (e.g., Okubo, 1986; Rothschild and Osborn, 1988; Yamazaki, 1993), as well as other areas in which turbulence is important (e.g., see McCave, 1984; Davis *et al.*, 1991; Yamazaki and Haury, 1993).

The view that turbulence is a homogeneous mixer of suspended particles is today inconsistent with the fact that turbulent flows are recognized to be characterized by structure and underlying coherence. This has been facilitated in part by the use of direct numerical simulation (DNS). Direct numerical simulations are computationally intensive and limited to relatively simple flows, but have become an increasingly powerful tool for improving our fundamental understanding of the dynamical and kinematical processes in turbulence. Because of the highly accurate techniques which may be employed in these calculations, numerical errors are small and DNS results may be analyzed in much the same fashion as data obtained from laboratory experiments or field measurements.

For marine applications, the important role of the underlying coherence and structure of turbulent flows has been given relatively little attention. Yamazaki (1993) considered the role of the organized nature of turbulent flows and its subsequent influence on the transport, evolution and concentration of planktonic organisms in the ocean. As discussed by Yamazaki (1993), the presence of coherent structures in turbulent flows must be important, since these structures have a spatial and temporal structure similar to algae and animals inhabiting the lower levels of the trophic pyramid. Yamazaki (1993) also argued that, while the effect of organized structures on particle transport was important, the degree to which turbulence influenced particle concentrations had not been quantified.

Relevant to studies of the effect of turbulence on marine particle transport is previous research which has demonstrated a preferential concentration of heavy particles (i.e., particles with large material densities relative to the surrounding fluid) by turbulence into regions of low vorticity or high strain rate (Squires and Eaton, 1991; Wang and Maxey, 1993). The work of Wang and Maxey (1993) is especially illuminating, since they have demonstrated the importance of small-scale fluid dynamics, i.e. effects of preferential concentration are the most pronounced for particle parameters comparable to the smallest scales, the Kolmogorov scales, of the flow.

Thus, it seems plausible that turbulence can have a significant effect on marine particle distributions. Furthermore, it may also be possible to estimate *a priori* the range of parameters, e.g., particle response time, diameter, etc., for which preferential concentration of marine particles could occur. However, unlike the studies of Squires and Eaton (1991) and Wang and Maxey (1993), particles encountered in marine and aquatic environments have material densities only slightly larger than that of the surrounding flow. The primary objective of the present contribution is to raise the issue of the importance of the coherent nature of small-scale turbulence and its effect on marine particle transport and preferential concentration.

A discussion of the parameter ranges in which preferential concentration may occur in marine and aquatic environments is presented in Section 2; also contained in that section is

an overview of the numerical simulations performed in this work. The results presented in Section 3 demonstrate that particles with material characteristics similar to marine particles can be strongly affected by turbulence. Implications of preferential concentration, a discussion on the limitations of the present study and directions for future research are then presented in Section 4.

2. BACKGROUND

2.1. *Preferential concentration of particles by turbulence*

Wang and Maxey (1993) studied the effect of turbulence on the settling velocity and concentration distribution of heavy particles in isotropic turbulence. One of the significant findings from their work was that preferential concentration of heavy particles follows Kolmogorov scaling, i.e., particles with parameters comparable to the Kolmogorov scales exhibit the greatest effects of preferential concentration. Thus, it is possible to estimate quantities such as the particle response time for which preferential concentration is significant. Of interest in this section is the use of Kolmogorov scaling to estimate parameters for which preferential concentration of marine particles may then be important.

For the sake of both parameter estimation as well as the numerical simulations presented in Section 3, marine particles are idealized as rigid spheres. This is a significant simplification since in general marine particles are both non-spherical and deformable. Thus, care must be exercised in estimation of particle parameters as discussed here as well as in interpretation of the results presented in Section 3. However, as discussed above, the principal goal of this study is to gain insight into preferential collection of marine particles in turbulent flows. Therefore, treatment of marine particles as rigid spheres is justified as a first approximation. For a rigid sphere in a non-uniform velocity field, the particle equation of motion is:

$$m_p \frac{\mathrm{d}\mathbf{v}}{\mathrm{d}t} = 6\pi a\mu\left(\mathbf{u} - \mathbf{v} + \frac{1}{6}a^2\nabla^2\mathbf{u}\right) + m_f\frac{\mathrm{D}\mathbf{u}}{\mathrm{D}t} + \frac{1}{2}m_f\left(\frac{\mathrm{D}\mathbf{u}}{\mathrm{D}t} - \frac{\mathrm{d}\mathbf{v}}{\mathrm{d}t} + \frac{\mathrm{d}\frac{1}{10}a^2\nabla^2\mathbf{u}}{\mathrm{d}t}\right) \tag{1}$$

$$+ 6\pi a^2\mu\int_{-\infty}^{t}\mathrm{d}\tau\frac{\mathrm{d}\mathbf{u}/\mathrm{d}\tau - \mathrm{d}\mathbf{v}/\tau + \mathrm{d}\frac{1}{6}a^2\nabla^2/\mathrm{d}\tau}{[\pi\nu(t-\tau)]^{1/2}} + \mathbf{g}(m_p - m_f) \tag{2}$$

(Maxey and Riley, 1983). In (2), $\mathbf{v}$ is the vector-valued particle velocity and $\mathbf{u}$ is the fluid velocity at the instantaneous particle position. The particle mass and fluid mass displaced by the particle are m_p and m_f, respectively. The particle radius is a and μ and ν are the dynamic and kinematic fluid viscosities, respectively. The acceleration of gravity is denoted $\mathbf{g}$ and the material derivative $\mathrm{D}/\mathrm{D}t$ is measured following the particle. The forces on the right-hand side of (2) correspond, in turn, to viscous drag, the pressure gradient in the undisturbed fluid, added mass effects of the form given by Auton *et al.* (1988), the Basset history force and gravity. It should be noted that the Basset force is derived for the case in which the Reynolds number based on particle radius and slip velocity is zero. Departures from this condition result in a more quickly decaying kernel of the Basset term. Therefore, in most practical applications, including the present work, it is justified to neglect this term (see Mei *et al.*, 1991 for further discussion).

Neglecting the Basset history term and Faxen corrections permits one to express (2) in a more compact form:

$$\frac{\mathrm{d}\mathbf{v}}{\mathrm{d}t} = \alpha[\mathbf{u} - \mathbf{v} - w\mathbf{e}_2] + \frac{3}{2}R\frac{\mathrm{D}\mathbf{u}}{\mathrm{D}t}, \tag{3}$$

(gravity is considered to act along the x_2 direction). As may be observed in (3), there are three parameters relevant to particle motion. The inertia parameter α, mass ratio parameter R, and settling velocity parameter w, defined as:

$$\alpha = \frac{6\pi a\mu}{m_p + \frac{1}{2}m_f}, \qquad R = \frac{m_f}{m_p + \frac{1}{2}m_f}, \qquad w = \frac{(m_p - m_f)g}{6\pi a\mu}. \tag{4}$$

The inertia parameter α reflects the relative importance of viscous to inertial effects and is significant for marine and aquatic applications in which viscous forces are important. The mass ratio parameter R reflects the difference in fluid and particle densities and the settling velocity parameter w represents the ratio of gravitational to viscous forces.

For heavy particle transport $m_p/m_f \gg 1$ and the last term of (3) is negligible since R is $\mathcal{O}(10^{-3})$ (e.g., see Squires and Eaton, 1991). For this class of flows, preferential concentration of particles by turbulence is the most significant when:

$$\alpha \approx 1/\tau_k, \qquad w \approx v_k. \tag{5}$$

In (5), τ_k and v_k are the Kolmogorov time and velocity scales, respectively, and are defined as:

$$\tau_k = \left(\frac{\nu}{\varepsilon}\right)^{1/2}, \qquad v_k = (\nu\varepsilon)^{1/4}. \tag{6}$$

where ε is the turbulence dissipation rate. Assuming that Kolmogorov scaling is applicable also for preferential concentration of marine particles, it is then possible using (4)–(6) to predict the particle parameters for which preferential concentration may be most significant. In the upper ocean, the turbulence dissipation rate ε varies over a wide range, i.e. from roughly 10^{-4} to 10^{-7} W kg^{-1} in the upper mixed layer and 10^{-7} to 10^{-10} W kg^{-1} in the seasonal thermocline (see Yamazaki and Osborn, 1988; Gargett, 1989). Thus, parameters such as response time and diameter for particles, which may be strongly affected by turbulence, will also vary. For example, the mass ratio of particles having a radius a of roughly 150 μm is approximately $m_p/m_f = 1.02$ (McCave, 1984). The inertia parameter α from (4) is then about 100 s^{-1}. Similarly, for particles with $a = 500$ μm, $m_p/m_f = 1.004$ (McCave, 1984) and the inertia parameter from (4) is roughly 10 s^{-1}. For a value of the dissipation rate in the upper mixed layer of 10^{-4} W kg^{-1} the Kolmogorov timescale from (6) is roughly 0.1 s. Thus, for particles in this size range $\alpha\tau_k$ varies from $10/\tau_k$ to $1/\tau_k$ and, based upon Kolmogorov scaling, these particles should be expected to exhibit effects of preferential concentration by turbulence. Furthermore, as also shown in McCave (1984), the settling velocities of these particles are order 1 mm s^{-1} which is comparable to v_k from (6) for $\varepsilon = 10^{-4}$ W kg^{-1}.

Using a similar analysis for the seasonal thermocline, with $\varepsilon = 10^{-7}$ W kg^{-1}, a variation of the inertia parameter from $10/\tau_k$ to $1/\tau_k$ corresponds to a variation in the particle radius a from roughly 1 to 3 mm, respectively. For particles in this size range the mass ratio m_p/m_f is approximately 1.003 (McCave, 1984). As also shown by McCave (1984) the settling

Table 1. *Flow field parameters*

ν	q^2	ε	L_f	Re_λ	$k_{\max}\eta$	$\Delta T/T_f$
0.00314	0.108	0.00346	0.942	42.4	1.24	5.11

velocity for particles in this size range is about 1.5 mm s^{-1}, which is roughly twice the velocity scale v_k from (6). Thus, for the upper range of dissipation rates encountered in the seasonal thermocline, strong interactions with the local turbulent flow field should be observed for particles in this size range.

2.2. *Simulation overview*

The effect of preferential concentration was investigated with DNS of the incompressible Navier–Stokes equations:

$$\frac{\partial \mathbf{u}}{\partial t} + \mathbf{u} \cdot \nabla \mathbf{u} = -\frac{1}{\rho_f} \nabla P + \nu \nabla^2 \mathbf{u}, \tag{7}$$

$$\nabla \cdot \mathbf{u} = 0. \tag{8}$$

In (7) and (8), $\mathbf{u}$ is the vector-valued velocity, P the fluid pressure, ν the kinematic viscosity, and ρ_f the fluid density. The governing equations (7) and (8) were solved by a pseudo-spectral method in which the dependent variables are represented by series expansions (Rogallo, 1981). The principal advantage of pseudo-spectral methods is that series expansions permit extremely accurate evaluation of spatial derivatives. In this method, the differential equations for the Fourier coefficients are time advanced using second-order Runge–Kutta; de-aliasing of the non-linear terms is accomplished through a novel combination of truncation and coordinate shifts. The flow field obtained through solution of (7) and (8) is represented directly on the computational grid, i.e., without resorting to *ad hoc* modeling of turbulent motions at any scale. Because of the rapid increase in the range of length scales with increasing Reynolds number, however, DNS is restricted to relatively low Reynolds number canonical flows.

The simulations performed in this study were of homogeneous, isotropic turbulence. A non-uniform body force was applied to the largest scales of motion in order to maintain a statistically stationary flow. The particular method used was developed by Hunt *et al.* (1987) in which a spatially non-uniform, time-independent body force is added to the Navier–Stokes equations at every time step. The flow field was resolved using 48^3 collocation points, corresponding to a maximum computational wavenumber of $(\sqrt{2}/3)48 = 23$ (the maximum computational wavenumber is dependent on the de-aliasing scheme; see Rogallo, 1981). The force field was applied to all modes with wavenumber magnitude $k \leqslant \sqrt{2}$.

The flow was started from an arbitrary initial condition and time advanced until it attained a statistically stationary state and retained no memory of its initial conditions. At this equilibrium condition, production of turbulence energy through the forcing scheme is exactly balanced by viscous dissipation. The hydrodynamic properties of the flow corresponding to the equilibrium condition are summarized in Table 1 (the quantities shown in the table are ensemble averages over the duration of the calculation). The

Table 2. Particle parameters

	α_k	R	w/v_k
Case 1	1.0	0.664	0.00
Case 2	1.0	0.664	1.25
Case 3	1.0	0.664	2.50
Case 4	2.0	0.664	1.25
Case 5	5.0	0.664	1.25
Case 6	10.0	0.664	1.25

Reynolds number, Re_λ, is based on the root-mean-square (rms) velocity fluctuation, $u' = \sqrt{q^2/3}$ and Taylor microscale, λ. For isotropic turbulence, λ is given by the relation:

$$\lambda = \left(\frac{5\nu}{\varepsilon}\right)^{1/2} q. \tag{9}$$

Twice the turbulence kinetic energy, q^2, and the viscous dissipation rate, ε, are determined from the three-dimensional energy spectrum:

$$\frac{1}{2}q^2 = \int E(k)\mathrm{d}k, \qquad \varepsilon = 2\nu \int k^2 E(k)\mathrm{d}k, \tag{10}$$

where k is the magnitude of the wavenumber vector $\mathbf{k}$. Also shown in Table 1 is $k_{\max}\eta$, where $k_{\max}$ is the maximum wavenumber of the simulation (defined previously) and η is the Kolmogorov length scale, $\eta = (\nu^3/\varepsilon)^{1/4}$. The duration of the simulations has been expressed in Table 1 in terms of the eddy turnover time, T_f, where T_f is defined in terms of the rms velocity fluctuation, u', and longitudinal integral scale, L_f, i.e., $T_f = L_f/u'$.

One of the primary difficulties associated with using numerical simulation to gain insight into marine particle transport are the limitations associated with DNS in general, i.e. low Reynolds number and a limited range of length scales resolved in the calculation. As discussed in Section 2.1, turbulence dissipation rates in the upper ocean span several orders of magnitude and only the lowest values can be captured by DNS. In this work, the governing equations were made dimensionless using a reference velocity scale $U_0 = 1$ cm s^{-1} and reference length scale $L_0 = 20/2\pi$ cm. These reference scales, together with a value for the kinematic viscosity of 0.01 $\mathrm{cm}^2\,\mathrm{s}^{-1}$, yield a dissipation rate in the DNS calculations of ε of 10^{-7} W kg^{-1}, which is a realistic value in the seasonal thermocline.

2.3. *Particle parameters*

As shown in Section 2.1, it is necessary to specify three parameters of particle motion, the inertia parameter α, the mass ratio parameter R and the settling velocity parameter w. The inertia parameter α was varied from $10/\tau_k$ to $1/\tau_k$ and the drift velocity was varied from 0 to $2.50v_k$ (Table 2). For the current simulations corresponding to a dissipation rate ε of approximately 10^{-7} W kg^{-1}, the Kolmogorov length, time and velocity scales are roughly 2 mm, 3 s and 0.60 mm s^{-1}, respectively. Referencing the inertia and settling velocity parameters to the Kolmogorov scales as in the current calculations results in variation of a from 1 to 3 mm and velocity w from 0 to 1.5 mm s^{-1}. The corresponding value of the mass ratio m_p/m_f for particles in this size range is about 1.003 (McCave, 1984). The resulting

value of R from (4) used in the simulations was 0.664. It should be remarked that, while these values for the particle parameters are representative of those encountered in marine settings (McCave, 1984) and, more importantly, correspond to particles with time and velocity scales similar to the Kolmogorov scales (for $\varepsilon = 10^{-7}$ W kg^{-1}), the particle diameters considered in the simulations are of the same order of magnitude as the Kolmogorov length scale η for simulations with $\alpha = 10/\tau_k$ and larger than η for simulations with $\alpha = 1/\tau_k$. The particle equation of motion is formally derived for particle diameters smaller than the Kolmogorov length scale. Results from application of (3) for the particles considered in the present simulations should, therefore, be treated with caution, since the effect of flow field non-uniformity may be important. However, correction of the equation of motion is beyond the scope of this work, and we believe that the qualitative nature of the findings obtained from the present study would not be significantly altered by the modification.

The trajectory of each particle was obtained through numerical integration of (3). Both (3) as well as the particle displacement were advanced using the same scheme as for the hydrodynamic field (second-order Runge–Kutta). Since it is only by chance that a particle will be located at a grid point where the turbulence is available, the fluid velocity at the particle position is obtained via trilinear interpolation. As has been shown by several investigators (e.g., see Squires and Eaton, 1991), trilinear interpolation is sufficiently accurate for resolution of lower-order statistics. In order to sufficiently resolve the number density field, the trajectories of 165,888 particles were tracked in the simulations, corresponding to an average number density of $165{,}888/48^3 = 1.5$ particles per computational cell. The particles were initially seeded at random locations throughout the computational domain; statistics of the particle cloud were obtained only after they had become independent of their initial conditions.

3. RESULTS

The turbulence velocity and vorticity vectors from a single plane of the three-dimensional computation are shown in Figs 1a and b, respectively. The x–z plane shown in Fig. 1 is from the final time step of the simulation. The plane shown is a representative snapshot of the vectors from other planes at different times and provides an illustration of the structure and coherence of even a simple flow such as isotropic turbulence. It should also be noted that the existence of structure in isotropic turbulence is not inconsistent with that of isotropy since coherence describes identifiable fluid motions in turbulent flows while isotropy is a statistical notion. Comparison of the three-dimensional energy spectrum of the fluid velocity from the DNS calculations with the data of Comte-Bellot and Corrsin (1971) is shown in Fig. 2. The experimental data were obtained downstream of a turbulence-generating grid in a wind tunnel. The spectra shown in Fig. 2 have been plotted in terms of Kolmogorov scaling, and it is evident that there is good agreement between the DNS data and experimental measurements.

Contours of the particle number density field for Cases 1–3 are shown in Fig. 3. The x–z plane shown in Fig. 3 is the same as in Fig. 1; the contour levels in each of the figures are also identical. It is apparent that the particles are not uniformly distributed throughout the volume and that there are distinct regions of particle accumulation. The peak number density for Case 1 is 25 times the global mean value, while for Cases 2 and 3 the peak number densities are 41 and 65 times the global mean, respectively. In Cases 1–3, the

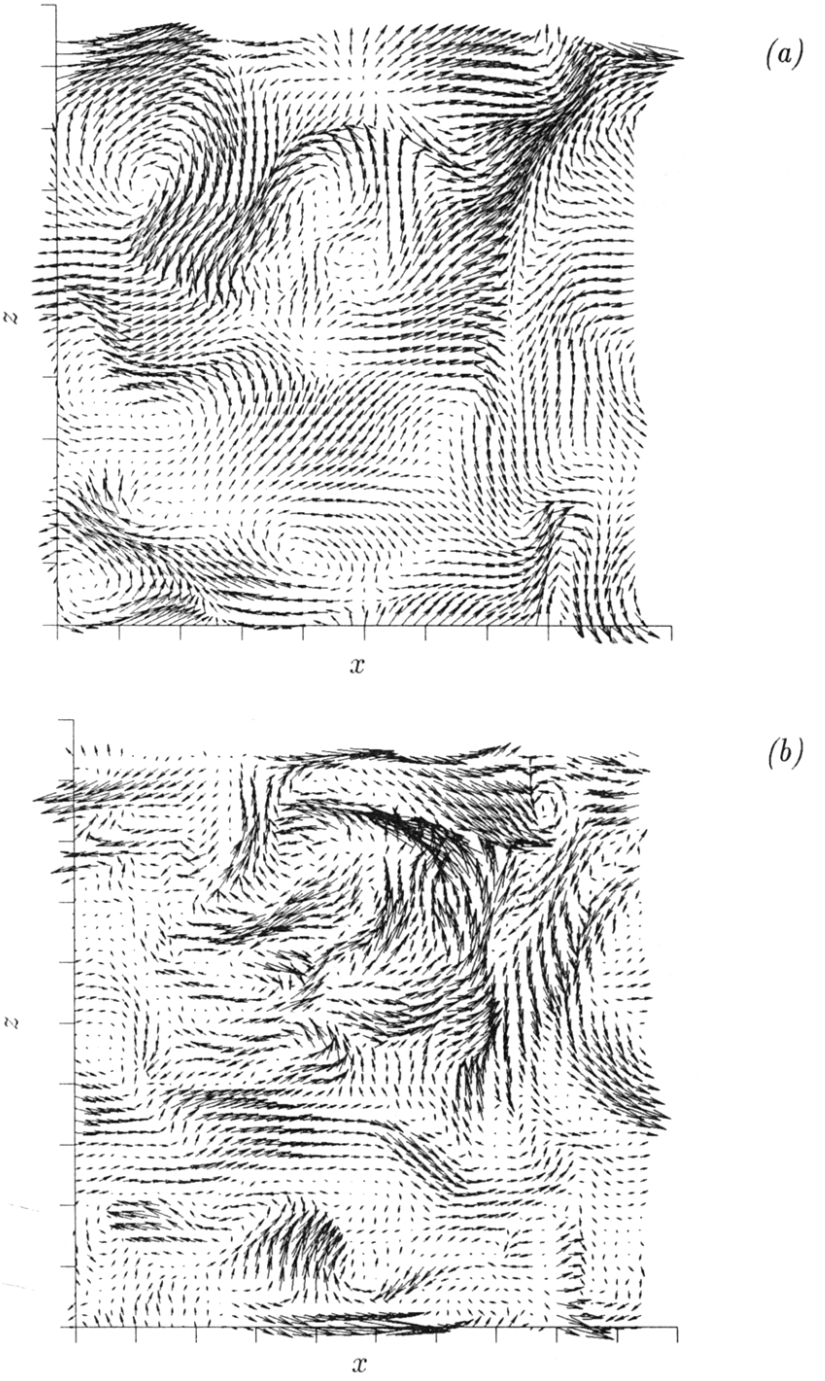

Fig. 1. Velocity vectors (*a*) and vorticity vectors (*b*) in an x–z plane ($y = \pi$) from the three-dimensional direct numerical simulation; vector length has been scaled by velocity magnitude in (*a*) and vorticity magnitude in (*b*). The computational domain is defined in the region $0 \leq x \leq 2\pi$.

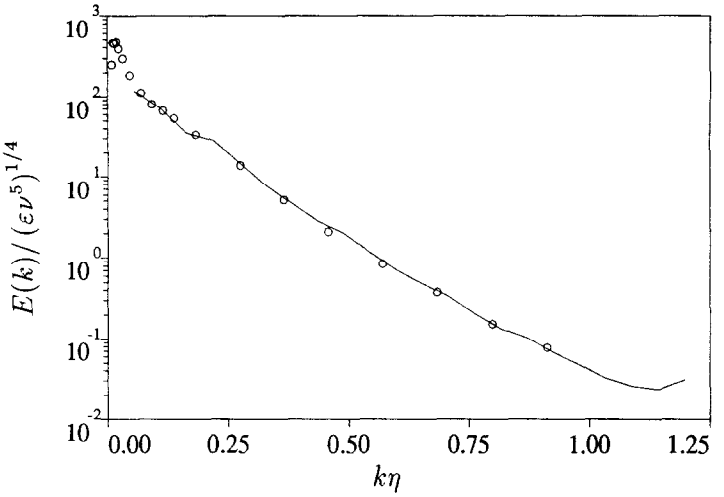

Fig. 2. Comparison of three-dimensional energy spectrum, $E(k)$, from DNS computation to experimental measurements of Comte-Bellot and Corrsin (1971), — DNS result; ○ exp. Experimental data obtained downstream of turbulence-generating grid (with 2-inch mesh spacing) at streamwise location $\bar{U}t/M = 98$ ($\bar{U}$ and M are the mean velocity and mesh spacing, respectively). Taylor-microscale Reynolds number in the experiment at this location is $Re_\lambda = 65.3$.

settling velocity parameter is increased for a fixed particle relaxation time. The increase in number density with increasing settling velocity is presumably linked to the phenomenon of preferential sweeping discussed by Wang and Maxey (1993). Preferential sweeping of particles arises from an inertial bias in the particle motion causing the particle to follow the downflow (in the direction of gravity) regions in a turbulent flow.

Similar effects of preferential concentration may be observed in Fig. 4. The number density contours shown in these figures are for Cases 4–6 and demonstrate the effect of variation in the particle inertia time for fixed settling velocity. The peak number densities for Cases 4, 5 and 6 are 20, 10 and 6 times the global mean value, respectively. Further, comparison of the number density field for varying values of the inertia parameter in Fig. 4 to Fig. 3b shows the most significant effects of preferential concentration occur for $\alpha\tau_k = 1$, consistent with the earlier work of Wang and Maxey (1993). It is also important to point out that particles with larger inertia parameters (i.e., smaller particles) also exhibit effects of preferential concentration, and the hydrodynamic influence of turbulence on particle distributions cannot be discounted.

It is possible to further quantify the results discussed above by examining the probability distribution function (pdf) of the particle number density field. Following Squires and Eaton (1991) and Wang and Maxey (1993), two pdfs have been used to quantify the effects of preferential concentration. The first pdf measures the probability that the number density in a computational cell is equal to a particular value c. This pdf is shown in Fig. 5. Also shown for comparison in the figure is the pdf resulting from a random distribution of particles throughout the computational domain, i.e. the Poisson distribution:

$$p_u(k) = \frac{e^{-\langle c\rangle}}{k!}\langle c\rangle^k. \tag{11}$$

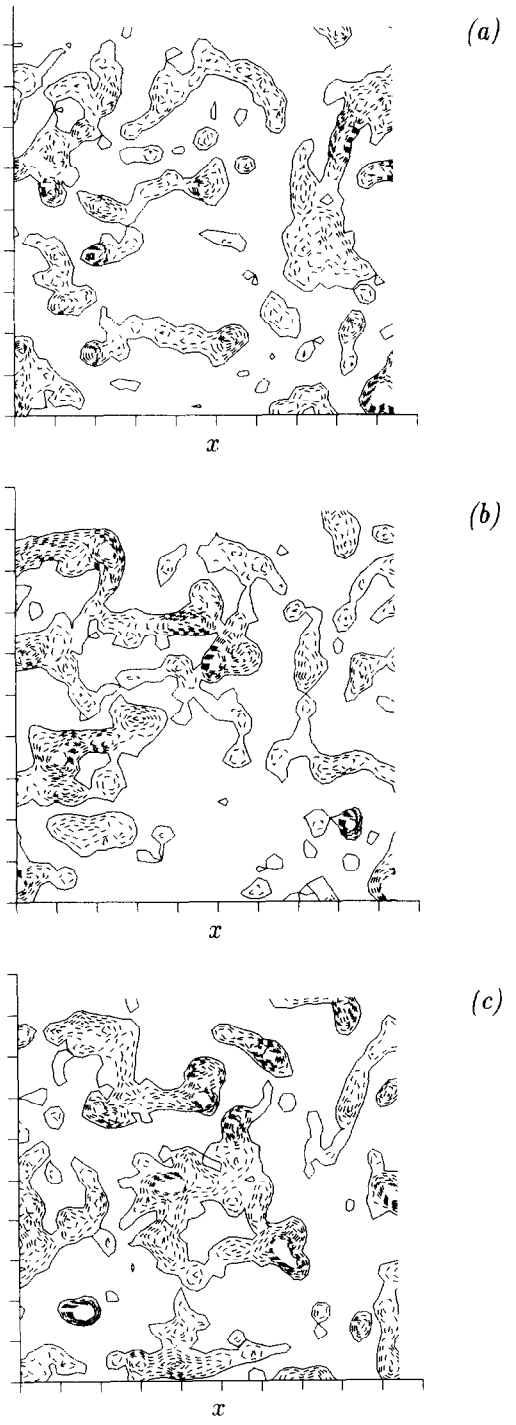

Fig. 3. Particle number density contours. The contour levels have been drawn from the global mean (solid line) to four times the mean value (dashed line). (*a*) Case 1, (*b*) Case 2, (*c*) Case 3.

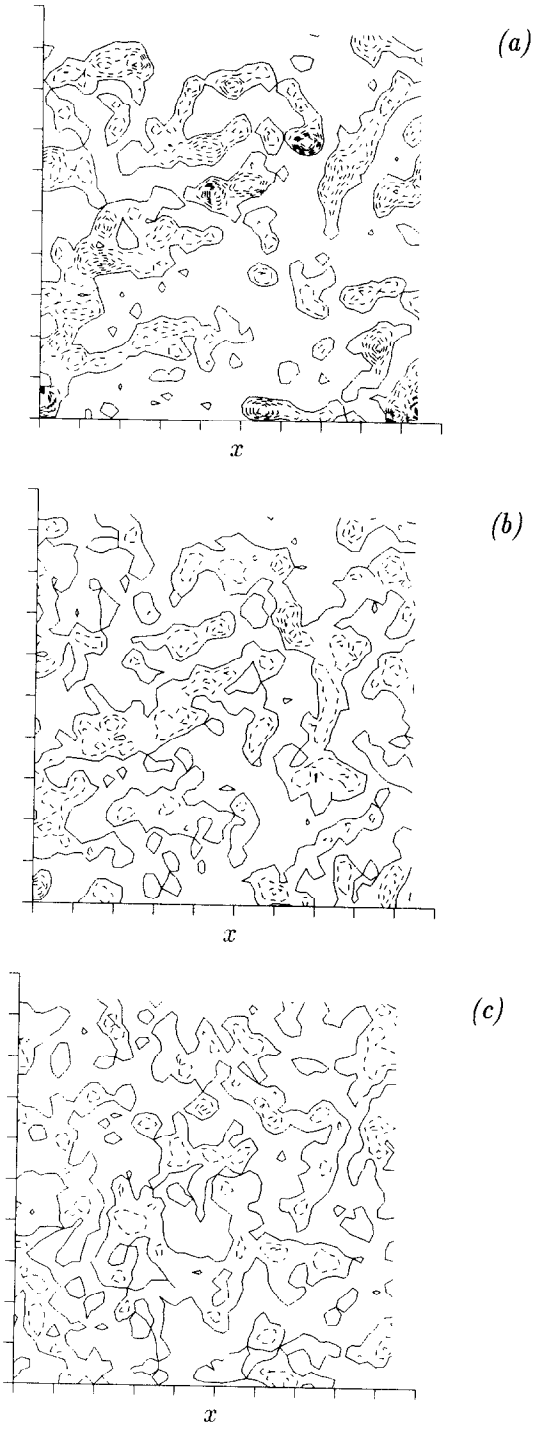

Fig. 4. Particle number density contours. The contour levels have been drawn from the global mean (solid line) to four times the mean value (dashed line). (*a*) Case 4, (*b*) Case 5, (*c*) Case 6.

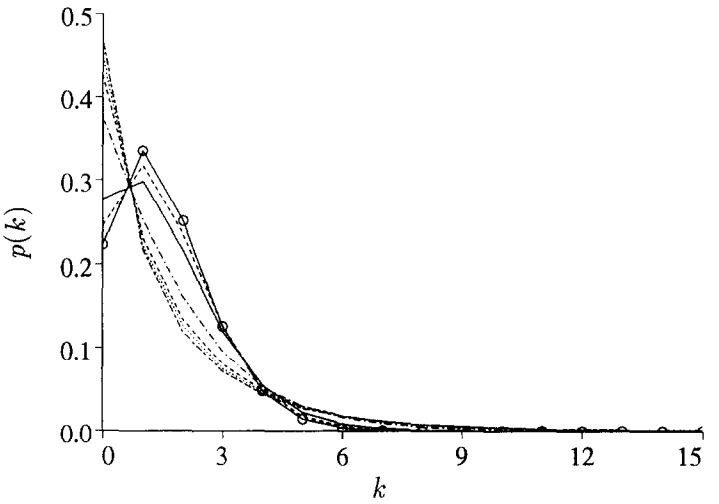

Fig. 5. Particle distribution $p(k)$ and comparison to random distribution. ⊖—⊖ random distribution; ---- Case 1; ------ Case 2; ——— Case 3; —·— Case 4; —— Case 5; ---- Case 6.

The mean number density in (11) is denoted $\langle c \rangle$ (= 1.5). The discrepancy between the measured pdfs and the Poisson distribution illustrates the non-uniformity of the number density field. For a random distribution approximately 22% of the computational cells are expected to be devoid of particles (for a mean number density of 1.5). Because of preferential concentration by turbulence, however, the fraction of the flow field devoid of particles is increased over the value predicted from a Poisson distribution. As can be observed from Fig. 5, the largest void fraction, 46%, occurs for Case 3 and is more than twice the value of the Poisson distribution. Furthermore, the probability of finding a computational cell containing two particles or less is 80% for Case 3. Since the total number of particles in the domain does not change with time, large void fractions imply that other regions of the flow will contain proportionally greater concentrations. This is evident from the pdfs shown in the figures; for values of k greater than about four, the measured pdfs are greater than the Poisson distribution. Thus, there are many more occurrences of cells containing high concentrations of particles than would be predicted from a random distribution.

Given the strong structural features of the number density field observed in both the contour plots as well as the pdfs shown in Fig. 5, it is also of interest to quantify the effects of preferential concentration using a pdf which measures the fraction of particles at those grid points where the concentration is a given value. This pdf was used by Wang and Maxey (1993) and relates the importance of a specific particle concentration in accounting for the total number of particles. This probability, $r(k)$, is related to the pdf $p(k)$ shown in Fig. 5 through:

$$r(k) = \frac{N_g}{N_p} kp(k), \tag{12}$$

where $N_g = 48^3$ and $N_p = 165{,}888$. The measured probability $r(k)$ for each of the cases

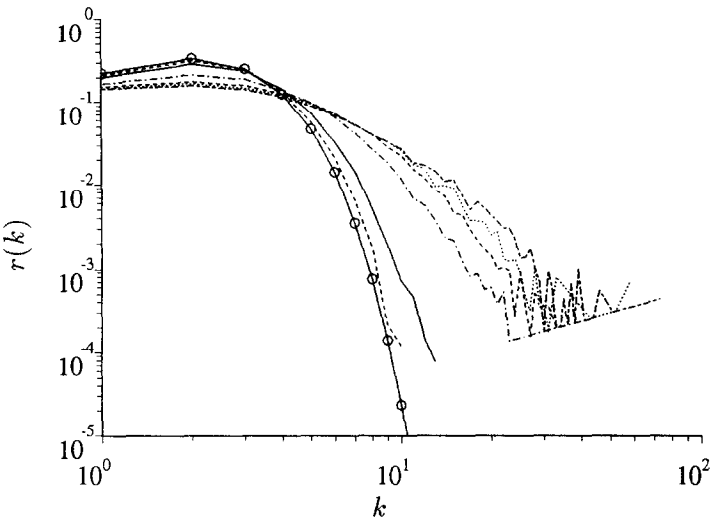

Fig. 6. Particle distribution $r(k)$ and comparison to random distribution. ⊖—⊖ random distribution; - - - - Case 1; - - - - - - Case 2; — — — Case 3; —·— Case 4; —— Case 5; — — — Case 6.

examined in this study is compared to the pdf for a random distribution in Fig. 6. As was the case with the pdfs in Fig. 5, there is significant difference between the measured pdfs and that corresponding to a random distribution of particles. As was observed in Fig. 5, 80% of the computational cells for Case 3 contain two particles or less. This is also nearly identical to the value for a random distribution. However, from Fig. 6 it may be observed that the cells containing two particles or less for Case 3 account for only 31% of the total number of particles (compared to 56% for a random distribution). Thus, the vast majority of particles are located in a small region of the domain where the concentration is significantly larger than the mean value. The spotty, intermittent nature of the number density field is thus quite analogous to the intermittent nature of the dissipation in homogeneous turbulence.

From the pdfs shown in Figs 5 and 6, a global measure of the effect of preferential concentration of particles can also be obtained. This measure is the integrated square deviation of each pdf:

$$D_p = \sum p(k) - p_u(k)^2, \tag{13}$$

$$D_r = \sum r(k) - r_u(k)^2 \tag{14}$$

and provides a measure of the variation from a random particle distribution. In (13) and (14), $p(k)$ and $r(k)$ are the measured values and $p_u(k)$ and $r_u(k)$ are the pdfs corresponding to a random distribution of particles. The advantage of the measures given by (13) and (14) is that both provide an integrated measure of the effect of preferential concentration as well as a measure which directly facilitates comparison of the various cases. Shown in

Table 3. D_p *and* D_r

	D_p	D_r
Case 1	6.840×10^{-2}	4.946×10^{-2}
Case 2	8.137×10^{-2}	5.584×10^{-2}
Case 3	9.294×10^{-2}	6.094×10^{-2}
Case 4	3.903×10^{-2}	2.948×10^{-3}
Case 5	5.605×10^{-3}	4.418×10^{-3}
Case 6	1.110×10^{-3}	8.117×10^{-4}

Table 3 are D_p and D_r. Consistent with the number density contours discussed above and the pdfs in Figs 5 and 6, both D_p and D_r show the effect of preferential concentration increases for smaller values of the inertia parameter and larger values of the settling velocity.

4. SUMMARY

Application of Kolmogorov scaling has been used to estimate parameters in which preferential concentration of marine particles may occur. Direct numerical simulations of isotropic turbulence were used to demonstrate that turbulence can produce a highly non-uniform particle number density field. The local particle number densities are as large as 10–60 times the global mean value. The pdfs of the particle number density showed that void fractions in the particle distributions are much larger than would be obtained for a random distribution of particles in the flow. Both the pdfs as well as integrated mean-square measures of the difference between the actual pdf and that corresponding to a random distribution show regions of significant preferential concentration; furthermore, these regions were also shown to account for a large fraction of the total population of particles. It is important to emphasize that these results, while obtained for particles representative of those encountered in marine and aquatic environments, are consistent with the previous findings for heavy particles obtained by Wang and Maxey (1993). This, in turn, further underscores the importance of their work, since the universality implied by Kolmogorov scaling of preferential concentration is not overly sensitive to particle and fluid densities.

There are several implications of preferential concentration of particles in marine and aquatic environments. For example, feeding experiments with calanoid copepods as grazers and algae as food have traditionally been performed in environments in which the influence of turbulence has not been considered. Whether the discrepancy in the clearance rate observed in these experiments (Strickler, 1985) is a result of copepods tracking local concentrations of food with mixed success is a question which can now be asked and, more importantly, answered. It is possible that preferential concentration will provide new perspectives in the research on secondary producers as well. In addition, the effect of non-random particle distributions may also have important effects on nonlinear concentration-dependent processes such as phytoplankton coagulation (e.g., Jackson and Lochmann, 1993) and the encounter of a mate during sexual reproduction (Waite and Harrison, 1992).

Thus, while the present work has addressed the importance of the coherent nature of small-scale turbulence on marine particle concentrations, the tendency of particles to exhibit preferential concentration as demonstrated in this study should be qualified in

several respects. The main sources of error are due to limitations of the turbulence simulations as well as deficiencies associated with the particle equation of motion. The numerical simulations represent the dynamics of incompressible turbulence in the dissipation range since the Reynolds number which can be accurately captured by DNS is low. This is a severe limitation, since the Reynolds numbers encountered in oceanic applications vary over a considerably larger range. Thus, the importance of scales much larger than can be accurately captured in DNS to particle transport remains to be evaluated through laboratory experiments and field measurements. The simulations were also of turbulence in which a steady force was applied to maintain a statistically stationary flow. Wang and Maxey (1993) have shown that similar features of local accumulation of heavy particles are observed when different forcing schemes are used and it is not expected that significant differences would be observed in this work using different forcing schemes (see also Ruetsch and Maxey, 1992).

Deficiencies associated with the particle equation of motion used in this work are another area in which the present approach is limited. As discussed in Section 2.1, marine particles are non-spherical and deformable but were idealized as rigid spheres in order to perform numerical simulations. Similar to the limitations imposed by DNS on the available Reynolds number range, the validity of this idealization awaits confirmation from laboratory experiments and field measurements. A more significant drawback is associated with the fact that marine particles which should exhibit preferential concentration (based on Kolmogorov scaling) have diameters comparable to the smallest scales of the flow. This, in turn, limits the applicability of the particle equation of motion, which is formally derived for particles smaller than the smallest scales of the turbulence. Effects of flow-field non-uniformity, neglected in the present study, as well as other effects such as non-linear drag, could have an important influence on particle motion. Despite these difficulties, it is hoped that this work marks the initial step towards an improved understanding of the interaction between marine particles and turbulence.

Acknowledgements—The authors are grateful for helpful comments on the manuscript by Professor J. Rudi Strickler as well as those of the referees. This work was supported by funding from the National Science Foundation (OCE-9016843, OCE-9213856, OCE-9409073) and Office of Naval Research (N00014-92-J-1653).

REFERENCES

Auton T. R., J. C. R. Hunt and M. Prud'homme (1988) The forces exerted on a body in inviscid unsteady non-uniform rotational flow. *Journal of Fluid Mechanics*, **197**, 241.

Comte-Bellot G. and S. Corrsin (1971) Simple Eulerian time correlation of full- and narrow-band velocity signals in grid-generated, 'isotropic' turbulence. *Journal of Fluid Mechanics*, **48**(2), 273.

Costello J. H., C. Marrase, J. R. Strickler, R. Zeller, A. J. Freise and G. Trager (1990) Grazing in a turbulent environment: I. Behavioral response of a calanoid copepod, Centropages hamatus. *Proceedings of the National Academy of Science, U.S.A.*, **87**, 1648–1652.

Davis C. S., G. R. Flierl, P. H. Wiebe and P. J. S. Franks (1991) Micropatchiness turbulence and recruitment in plankton. *Journal of Marine Research*, **49**, 109–151.

Gargett A. E. (1989) Ocean turbulence. *Annual Review of Fluid Mechanics*, **21**, 419–451.

Granata T. C. and T. D. Dickey (1991) The fluid mechanics of copepod feeding in a turbulent flow: a theoretical approach. *Progress in Oceanography*, **26**, 243–261.

Hunt J. C. R., J. C. Buell and A. A. Wray (1987) Big whorls carry little whorls. *Proceedings of the* 1987 *Summer Program*. Report CTR-S87, NASA/Stanford Center for Turbulence Research.

Jackson G. A. and S. E. Lochmann (1993) In: *Environmental particles*, J. Buffle and H. P. van Leeuwen, editors, Lewis Publishers.

Kiørboe T. (1993) Turbulence, phytoplankton cell size and the structure of pelagic food webs. *Advances in Marine Biology*, **29**, 2.

Madden C. J. and J. W. Day (1992) Induced turbulence in rotating bottles affects phytoplankton productivity measurements in turbid waters. *Journal of Plankton Research*, **14**, 1171–1191.

Mann K. H. and J. R. N. Lazier (1991) *Dynamics of marine ecosystems*. Blackwell Scientific Publications, Boston.

Marrase C., J. H. Costello, T. Granata and J. R. Strickler (1990) Grazing in a turbulent environment: II. Energy dissipation encounter rates and efficacy of feeding currents in *Centropages hamatus*. *Proceedings of the National Academy of Science, U.S.A.*, **87**, 1653–1657.

Maxey M. R. and J. J. Riley (1983) Equation of motion for a small rigid sphere in a nonuniform flow. *Physics of Fluids*, **26**, 883.

McCave I. N. (1984) Size-spectra and aggregation of suspended particles in the deep ocean. *Deep-Sea Research*, **22**, 491–502.

Mei R., C. J. Lawrence and R. J. Adrian (1991) Unsteady drag on a sphere at finite Reynolds number with small fluctuations in the free-stream velocity. *Journal of Fluid Mechanics*, **233**, 613.

Okubo A. (1986) Dynamical aspects of animal grouping: swarms, schools, flocks, and herds. *Advances in Biophysics*, **22**, 1–94.

Rogallo R. S. (1981) Numerical experiments in homogeneous turbulence. NASA TM 81315.

Rothschild B. J. and T. Osborn (1988) Small-scale turbulence and planktonic contact rates. *Journal of Plankton Research*, **10**, 465–474.

Ruetsch G. R. and M. R. Maxey (1992) The evolution of small-scale structures in homogeneous isotropic turbulence. *Physics of Fluids*, **4**, 2747.

Squires K. D. and J. K. Eaton (1991) Preferential concentration of particles by turbulence. *Physics of Fluids*, **3**, 1169.

Strickler J. R. (1985) Feeding currents in calanoid copepods: two new hypotheses. *Symposium for the Society of Experimental Biology*, **39**, 459–485.

Waite A. and P. J. Harrison (1992) Role of sinking and ascent during sexual reproduction in the marine diatom *Ditylum brightwellii*. *Marine Ecology Program Series*, **87**, 113–122.

Wang L.-P. and M. R. Maxey (1993) Settling velocity and concentration distribution of heavy particles in homogeneous isotropic turbulence. *Journal of Fluid Mechanics*, **256**, 27–68.

Yamazaki H. (1993) Lagrangian study of planktonic organisms: perspectives. *Bulletin of Marine Science*, **53**, 265–278.

Yamazaki H. and L. Haury (1993) A new Lagrangian model to study animal aggregation. *Ecological Modelling*, **69**, 99–111.

Yamazaki H. and D. Kamykowski (1991) The vertical trajectories of motile phytoplankton in a wind-mixed water column. *Deep Sea Research*, **38**, 219–241.

Yamazaki H. and T. R. Osborn (1988) Review of oceanic turbulence: implication for biodynamics. In: *Toward a theory on biological–physical interactions in the world ocean*, B. J. Rothschild, editor, Kluwer Academic Publishers, Dordrecht, pp. 215–233.